



11 **Abstract**

12 In the prospect of limited energy resources and climate change, effects of alternative biofuels on primary emissions  
13 are being extensively studied. Our two recent studies have shown that biodiesel fuel composition has a significant  
14 impact on primary particulate matter emissions. It was also shown that particulate matter caused by biodiesels was  
15 substantially different from the emissions due to petroleum diesel. Emissions appeared to have higher oxidative  
16 potential with the increase in oxygen content and decrease of carbon chain length and unsaturation levels of fuel  
17 molecules. Overall, both studies concluded that chemical composition of biodiesel is more important than its  
18 physical properties in controlling exhaust particle emissions. This suggests that the atmospheric aging processes,  
19 including secondary organic aerosol formation, of emissions from different fuels will be different as well. In this  
20 study, measurements were conducted on a modern common-rail diesel engine. To get more information on realistic  
21 properties of tested biodiesel particulate matter once they are released into the atmosphere, particulate matter was  
22 exposed to atmospheric oxidants, ozone and ultra-violet light; and the change in their properties was monitored for  
23 different biodiesel blends. Upon the exposure to oxidative agents, the chemical composition of the exhaust changes.  
24 It triggers the cascade of photochemical reactions resulting in the partitioning of semi-volatile compounds between  
25 the gas and particulate phase. In most of the cases, aging lead to the increase in volatility and oxidative potential,  
26 and the increment of change was mainly dependent on the chemical composition of fuels as the leading cause for the  
27 amount and the type of semi-volatile compounds present in the exhaust.

28

## 29 1. Introduction

30 In the urban environments the most significant contributor to the overall PM burden are traffic emissions (Pey et al.,  
31 2009). Harmful effects of DPM to humans and the environment have been extensively studied which resulted in the  
32 classification of Diesel Exhaust (DE) as carcinogenic by International Agency for Research on Cancer (IARC)  
33 (World Health Organization, 2013) in 2013. Following this, environmental agencies will tend to implement more  
34 stringent regulations to meet air quality standards forcing engine manufacturers to further reduce engine emissions.  
35 As biodiesel produces significantly less particulate matter (Surawski et al., 2013;Fontaras et al., 2009;Rahman et al.,  
36 2014) along with other economical and environmental advantages(Tinsdale et al., 2010;Kalligeros et al.,  
37 2003;Cheng et al., 2008); it may be the available option of the fuel industry in reducing PM emissions.  
38 Numerous studies reported the decrease in some controlled emissions with the usage of biodiesel (Bagley et al.,  
39 1998;Kalligeros et al., 2003;Knothe et al., 2006;Surawski et al., 2013;Rahman et al., 2014). It is also well  
40 established that biodiesel decreases black carbon emissions and increases the Soluble Organic Fraction (SOF)  
41 (Rahman et al., 2014;Sidhu et al., 2001). The decrease in particle emissions is also very often followed by the  
42 emission of smaller particles (Surawski et al., 2013), while the increase in SOF results in excessive amount of  
43 volatile and semi-volatile matter in the exhaust (Sidhu et al., 2001;Liu et al., 2008;Surawski et al., 2011). Both the  
44 decrease in particle size and the increase in SOF are believed to be linked to the increase of OP of particles (Biswas  
45 et al., 2009;Surawski et al., 2011).

46 People in urban and semi-urban environments are mainly exposed to a combination of fresh and aged primary  
47 emissions and SOA. The generation of SOA occurs during aging of primary emissions, mainly through oxidation of  
48 gas-phase organic compounds that can result either in the formation of new particles or condensation of these  
49 compounds onto pre-existing particles (Zielinska, 2005;Jathar et al., 2013). Consequently, atmospheric fate or aging  
50 of diesel exhaust has become of a great scientific interest and attracts significant attention from the researchers  
51 (Chirico et al., 2010;Leskinen et al., 2007;Miracolo et al., 2011;Miracolo et al., 2010;Nakao et al., 2011;Samy and  
52 Zielinska, 2010;Verma et al., 2009;Wang et al., 2011;Weitkamp et al., 2007). Although there are several studies on  
53 the aging of diesel exhaust, (Geiger et al., 2002;Lee et al., 2004;Leskinen et al., 2007;Robinson et al.,  
54 2007;Weitkamp et al., 2007;Li et al., 2009;Chirico et al., 2010;Miracolo et al., 2010;Nakao et al., 2011;Jathar et al.,  
55 2013), still a number of questions remained unanswered. Given the fact that biodiesel produces more of semi-

56 volatile matter and thus the contribution of biodiesels to SOA formation in urban environments could be significant,  
57 the atmospheric aging of biodiesel exhaust is yet to be explored in more detail.

58 Smog chambers are extensively used to conduct aging experiments on anthropogenic aerosols and investigate their  
59 potential to form SOA (Izumi and Fukuyama, 1990;Atkinson et al., 1980;Sidhu et al., 2001). Recently, flow-through  
60 reactors are drawing a great deal of attention for their advantages over smog chambers. While the use of smog-  
61 chambers to study the photochemical aging processes (Chirico et al., 2010;Leskinen et al., 2007;Miracolo et al.,  
62 2011;Miracolo et al., 2010;Nakao et al., 2011;Samy and Zielinska, 2010;Verma et al., 2009;Wang et al.,  
63 2011;Weitkamp et al., 2007) has been shown to be a valuable tool, there are some significant disadvantages  
64 associated with their usage. Their size, complexity, high cost and operational time required (typically only one  
65 experiment per day) make them impractical when series of experiments need to be conducted. As an alternative to  
66 smog chambers, flow-through reactors or “Potential Aerosol Mass” (PAM) chambers are becoming very popular  
67 among researchers (Kang et al., 2007;Lambe et al., 2011;Keller and Burtscher, 2012). PAM chambers simulate  
68 atmospheric photo oxidation processes. Employment of PAM chambers is associated with high oxidant  
69 concentrations and short exposure times mimicking few hours to few days of real-time atmospheric oxidation. The  
70 short residence time of PAM chambers further enables better control of the oxidant concentrations and minimizes  
71 wall losses, which could be significant in smog chambers (Kang et al., 2007).Also the response time in PAM  
72 chambers is by far less than that of smog chambers making it easier to observe the effect of changing a control  
73 variable. Moreover, experiments carried out on PAM chambers tend to be more repeatable and more reproducible  
74 (Kang et al., 2007).

75 So far, the PAM chambers have been used to investigate the potential of combustion generated aerosols to produce  
76 SOA including biomass burning (Keller and Burtscher, 2012) and 2-stroke engine exhaust (McWhinney et al.,  
77 2011). The potential of biodiesel exhaust gases to cause SOA formation is yet to be studied.

78 This research investigates the change in volatile organic content and the potential toxicity of biodiesel exhaust  
79 particulate matter after aging in a flow-through reactor. We explore the contribution of photochemical aging  
80 processes on the potential transfer of the semi-volatile fraction of biodiesel exhaust from the gas phase to the particle  
81 phase and the extent to which semi-volatile compounds are related to chemically active molecules that contain  
82 oxygen or Reactive Oxygen Species (ROS). The study, also aims to find a correlation between the chemical  
83 composition of biodiesel and the volatility and toxicity of biodiesel particulate matter while undergoing simulated  
84 aging processes. Specifically the main objective of this work is to critically examine the influence of the carbon

85 chain length, saturation levels and oxygen content of biodiesel Fatty Acid Methyl Ester (FAME) fuel molecules. All  
86 the work has been undertaken by investigating particle emissions from a common-rail engine using four palm oil  
87 biodiesels at different blend percentages.

## 88 **2. Experimental setup and methodology**

89 Figure 1 illustrates the experimental setup. The setup was composed of an existing EURO III diesel engine which  
90 was mounted on an engine dynamometer within the Biofuels Engine Research Facility (BERF) at Queensland  
91 University of Technology (QUT), and was used as the test bed. The engine was a 6-cylinder, turbo-charged,  
92 common-rail, Euro III, compression ignition engine with the displacement volume of 5.9 litres. More details of the  
93 experimental setup, engine specifications, dilution system along with the chemical and physical properties of fuels  
94 used can be found in our previous publication (Rahman et al., 2014). The main addition was that the diluted exhaust  
95 was passed through a flow-through reactor (PAM reactor) where the diluted exhaust is mixed with ozone and  
96 irradiated with UV light.

97 The flow-through-reactor was a 1-meter-long stainless steel cylinder which had four inlet ports and four outlet ports.  
98 There were also four lengthwise sampling points to enable measurement along the reactor length. In the centre of the  
99 reactor, there was space for a UV tube to irradiate the diesel exhaust. Considering the dimensions of the reactor, the  
100 UV tube as well as the flow rate through the reactor ( $7\pm 0.5$  lpm), the residence time (treatment time) of the reactor  
101 was estimated to be  $60\pm 10$  seconds. The amount of time the exhaust gas was exposed to simulated atmospheric  
102 conditions was much less than in the real conditions therefore the concentration of ozone and exposure to UV had to  
103 be higher compared to real atmospheric conditions. Based on a previous literature, this residence time approximately  
104 correlated to an exposure of at least 2 to 8 hours in the atmosphere (McWhinney et al., 2011). After aging in the  
105 reactor, diesel exhaust went to a number of different devices capable of measuring a variety of physical and  
106 chemical properties of gases and particles which will be explained later.

107 Purified air was drawn through the ozone generator (Ozonizer HLO 800) and was injected into the reactor where it  
108 was mixed with diluted and cooled diesel exhaust. The flow rate through the ozone generator was restricted using a  
109 critical orifice and was measured to be  $0.15$  lpm. To continuously monitor the concentration of ozone in the reactor  
110 an Echotech EC9810 Ozone Analyser was used. The average concentration of ozone in the reactor was kept to be  
111 around  $0.5\pm 0.1$  ppm during aging experiments. OH radical formation was not monitored and reported as this was a  
112 qualitative study showing the general effect without the quantification of SOA yields.

113 As mentioned before, to simulate sunlight and reactions induced by the irradiation of UV from the sun (Kang et al.,  
114 2007;Keller and Burtcher, 2012), there was a space for a UV tube in the centre of the reactor which was suitable to  
115 fit different types of UV light tubes (UV-A, UV-B and UV-C). The UV tube which was used in this study mostly  
116 emitted UV light at 253nm wave length (UVC).

117 A standard set of gas analyser was used to continuously monitor the concentrations of CO, CO<sub>2</sub> and NO<sub>x</sub>. More  
118 details on the gas analyser set is described in a recent publication (Rahman et al., 2014) .

119 Using a TSI Dustrak (model 8530) and applying the procedure proposed by Jamriska {Jamriska, 2004 #323}the  
120 mass concentration of particles were estimated and was used to normalize the ROS levels of the diesel exhaust. A  
121 Scanning Mobility Particle Sizer (SMPS TSI 3080, with a 3022 CPC) measured the size distribution of diesel  
122 exhaust. A Volatility Tandem Differential Mobility Analyser (VTDMA) consisting of an electrostatic classifier, a  
123 thermo-denuder and an SMPS (in-house designed column with a 3010 CPC) measured the amount of volatile matter  
124 in the diesel exhaust particles (Johnson et al., 2008). The VTDMA yielded the change in the diameter of particles for  
125 six pre-selected sizes: 30, 60, 90, 120, 150, 200 and 220 nm after they have passed through the thermo-denuder with  
126 the temperature set at 300° C. Using the VTDMA method, the volatility of particles was compared before and after  
127 aging in the reactor. The error range for the particle sizing instruments was less than 1 percent that led to a  
128 maximum 3% error for the volatility measurements (Pourkhesalian et al., 2014).

129 To measure the ROS levels of diesel exhaust of different fuel stocks before and after aging, the BPEA molecular  
130 probe (bis(phenylethynyl) anthracene-nitroxide) was applied in-situ. Samples were collected by bubbling aerosol  
131 through an impinger containing 20 mL of 4 µM BPEA solution which used an AR grade dimethylsulphoxide as the  
132 solvent. More details on the ROS sampling methodology, theory behind its application and proof of concept in the  
133 case of various combustion sources can be found in previous publications (Miljevic et al., 2010;Stevanovic et al.,  
134 2012a;Stevanovic et al., 2013;Miljevic et al., 2009;Stevanovic et al., 2012b).

## 135 **2.1. Fuel Selection**

136 In this study four FAME fuels with controlled chemical compositions were tested and compared to petro-diesel. The  
137 fuels differed in terms of iodine value and saponification value which correspond to saturation degree and oxygen  
138 content of the fuels respectively. To differentiate the effects caused by change of saturation degree from those  
139 caused by oxygen content, two of the biodiesels had very close saturation levels but different carbon chain lengths,  
140 while the other two biodiesels were the same in terms of oxygen content but different in saturation levels. We used

141 commercial petro-diesel to make 20% and 50% biodiesel blends. The FAMEs are labeled as C810, C1214, C1618  
142 and C1875, based on the number of carbon atoms in the most abundant fatty acid in that particular biodiesel stock.  
143 Some of the most important chemical and physical prosperities of the fuels can be found in a previous study by  
144 Rahman et al (Rahman et al., 2014).

## 145 **2.2. Operation of the engine**

146 Blends of 100%, 50%, 20% and 0% of biodiesel, noted as B100 (pure biodiesel), B50 and B20 and B0 (pure petro-  
147 diesel) respectively, were used to run the engine. All the tests were conducted at quarter load and at the engine speed  
148 of 1500 rpm. Tests were not done at several different loads and speeds to avoid too many variables. This test was  
149 designed to isolate the influence of changing fuel composition on the aging potential and related physico-chemical  
150 changes in PM.

## 151 **3. Results and discussion**

### 152 **3.1. Volatility measurements**

153 Figure 2 shows the change in Volumetric Volatile Fraction (VVF) of particulate component before and after  
154 exposure to UV light and ozone. A possible increase of volatile content of the particles after the exposure to  
155 oxidative agents can be seen in the figure. As the vapor pressure of the gases reduces due to photochemical  
156 reactions, some of the volatile substances partition from the gas phase into the particle phase resulting in more  
157 volatile particles(Leskinen et al., 2007;Donahue et al., 2006;Kroll and Seinfeld, 2008). It was observed that the  
158 exposure to oxidative agents did not lead to the formation of nucleation mode particles. It is to be noted that in cases  
159 when the dilution ratio is low and there is not enough surfaces available for the partitioning gas to condense on (e.g.  
160 application of diesel particulate filters), then formation of nucleation mode particles can occur (Lipsky and  
161 Robinson, 2006), but at high levels of dilution, semi-volatile compounds tend to partition in the gas phase (Robinson  
162 et al., 2007). The reason why we did not observe any nucleation mode particles was that the dilution ratio was rather  
163 large at more than 400 and there was no diesel particulate filter in use, so there were already surfaces available for  
164 the condensation of gaseous matter. (Shi and Harrison, 1999;Rönkkö et al., 2006)

165 In Figure 2, it can be seen that the volatility of particles has increased with the increase of biodiesel percentage in the  
166 blends (Pourkhesalian et al., 2014). While for B20, the amount of volatile matter is quite close to that of B0; the volatility  
167 of particles has increased considerably with B50 and B100. These findings were in a good agreement with the previous

168 observations, which showed a significant increase in volatility of diesel particulate matter with increasing biodiesel  
169 percentage in the blend (Pourkhesalian et al., 2014; Surawski et al., 2011). Particles produced by the combustion of C810  
170 and C1214 were the most volatile; also the change in volatility of these particles was more significant with increasing  
171 percentage of biodiesel in the blend; whereas, the change in volatility was almost negligible for C1875 and all of its blends  
172 which was the most unsaturated biodiesel with the longest carbon chain length and lowest oxygen content.

173 The effect of oxygen content on the volatility of particles with gaseous and liquid diesel fuels was studied previously  
174 (Sidhu et al., 2001; Xu et al., 2013; Pourkhesalian et al., 2014) and in our study, the increase of volatile matter in particles is  
175 more significant for more saturated fuels and with more oxygen content; where for C1875 the increase is just within the  
176 error range of the instrument.

177 The volatile fraction and the growth of volatile fraction for 30 nm particles were the largest in almost all cases which  
178 showed that more attention is to be paid to smaller particles; not only because of their ability to suspend longer and  
179 penetrate deeper in the lung (Sidhu et al., 2001; Liu et al., 2008; Surawski et al., 2011; Cheung et al., 2009), but also because  
180 of their probability of carrying more oxidized volatile organics as they age.

181 In B0, apart from 30 nm particles, for all other particle sizes, the amount of volatile matter is within the error range of the  
182 differential mobility analyzer (DMA), implying that B0 emits particles that are mainly composed of soot. Also after aging  
183 experiments, the increase in volatile fraction in B0 particles was just small enough to be neglected showing that either the  
184 amount of volatile matter in the gas phase is very small or they do not undergo photochemical reactions.

185 To be able to compare cases more easily, we have estimated the total amount of volatile matter that is in the liquid phase  
186 for each case and we called it Overall Volatility (OV). To do so, particles are assumed to be spherical. The volume of  
187 volatile matter is estimated using VTDMA data and the number concentration of each pre-selection size from SMPS data.  
188 The quantity, OV, is expressed through percentage and means that a certain proportion of the PM in the aerosol is  
189 composed of volatile matter while the rest is non-volatile (mainly elemental carbon) (Giechaskiel et al., 2009). More details  
190 of the concept and the procedure of estimating OV can be found in our recent study (Pourkhesalian et al., 2014).

191 Figure 3 illustrates the OV of diesel exhaust versus blend for different biodiesel and compared to petro-diesel. As  
192 previously observed (Surawski et al., 2011), the volatility of diesel particulate matter increases as the percentage of  
193 biodiesel goes higher in the blends. This fact is particularly seen in more saturated fuels with higher oxygen content. Blends



194 of C810 and C1214, which have short carbon chain lengths and high saturation degree, have produced emissions with the  
195 most volatile PM; while C1618 and C1875, with longer carbon chain lengths and more carbon double bonds (more  
196 saturated fuels), have produced less and less volatile PM. This can be explained by assuming that the oxygen borne with the  
197 molecule of the fuel can cause more oxidized combustion products being of low volatility both in the liquid phase and in  
198 the gas phase. Those volatile substances having a lower vapor pressure would condense on soot particles just after the  
199 combustion while in the combustion chamber or in the exhaust system, causing the volatile fraction of particle become  
200 more significant. The volatile fraction of particles produced by more oxygenated fuels increases more after aging because  
201 there are more semi-volatile and volatile matter in the gas phase undergoing photo chemical reactions and transforming into  
202 the particle phase and condensing onto the primary particles.

203 The two heavier biodiesel fuels which were tested in the study (C1618 and C1875) are more unsaturated, less oxygenated  
204 and have a longer carbon chain length and thus are more comparable to petro-diesel. Both of them caused more volatile PM  
205 comparing to B0 and their increase in volatility was not as significant as the two other biodiesel fuels in this study

206 PM due to short-length hydrocarbons blends (C810 and C1214) was more volatile before, but also after the aging process.

207 It can be seen that the carbon chain length of the fuel was a more influential factor on the volatility of PM than saturation  
208 degree of the fuel. The reason would be the fact that when the carbon chain length is shorter, the weight ratio of oxygen  
209 borne by the fuel molecule will be higher and thus more oxidative agent is available for the organics, so the vapor pressure  
210 of the products, whether before or after the exposure, will be further lowered as a result of oxidization. To examine this  
211 supposition, the oxygen content of all the fuels and blends were either measured or calculated, and then the change in the  
212 volatility of PM emitted by each blend (after aging) was plotted against the oxygen content of the blends (Figure 4). The  
213 effect of oxygen content of the blend on the increase of the volatile matter in the DPM is evident. Apart from two points  
214 (C1618, B100 and C1875, B100) that show low volatility with higher oxygen content; all other blends showed a good  
215 correlation between volatility and oxygen content.

216 The correlations between the variables were analyzed using the linear regression or generalized linear model with a log link  
217 function. The validation of model assumptions was performed by the residuals versus fit values and QQ plots. Modeling  
218 and visualizations were carried out using the ggplot2 package in R (Wickham, 2009)

### 219 **3.2. ROS measurements**

220 Oxidative potential measurement, expressed through ROS concentration of PM can be used as a good estimate for its  
221 reactivity and toxicity. An in-house developed profluorescent molecular probe BPEAnit was applied in an entirely novel,  
222 rapid and non-cell based way to assess particulate oxidative potential. Based on the data provided in the literature so far  
223 (Stevanovic et al., 2013), there are some uncertainties related to the nature of chemical species responsible for the measured  
224 redox potential and overall toxicity. However, the majority of research in this field reported that organic fraction, more  
225 precisely semi-volatile organic content, is in a good correlation with ROS concentration (Biswas et al., 2009;Miljevic et al.,  
226 2010;Surawski et al., 2011)

227 Figure 5 illustrates the oxidative potential of particles for all three biodiesel blends at 25% load, 1500 rpm before and after  
228 the aging process. The points corresponding to B0 are repeatedly presented in all blends to ease comparison of petro-diesel  
229 particulate oxidative potential with that of other blends. It is evident that aging process increases potential toxicity of  
230 particles by increasing ROS concentration in the case of all four biodiesel as well as petro-diesel. This result is supported  
231 by volatility measurements. As stated above, particles become more volatile after aging as a result of oxidation of semi-  
232 volatile compounds and their subsequent condensation onto pre-existing particles.

233 In Figure 5, the change in ROS content after exposure to UV and ozone is the most significant in the case of B100, and this  
234 increase in oxidative potential decreases with the decreasing percentage of biodiesels in blends. To further explore this, the  
235 change in ROS concentration was plotted against oxygen content of the fuels. A possible trend between the fuel oxygen  
236 content and ROS concentration is evident from Figure 6. The actual mechanism standing behind this aging transformation  
237 and subsequent partitioning remains unclear and is subject to further investigation. However, this graph is showing an  
238 indication that the amount of increased ROS concentration upon oxidative aging is more significant in the case of PM  
239 originating from the combustion of molecules with higher oxygen content. To get a further insight into the aging process of  
240 tested aerosols, the oxidative potential of the gas phase was measured as well. The results are summarised in Figure 7 and  
241 they show interesting trends. When the compounds from the gas phase are oxidized they are transferred into the particle  
242 phase due to the decrease of their saturation vapor pressure. In this case one would expect a decrease in the concentration of  
243 the gaseous component after aging. This is the case with long chain, unsaturated biodiesels- C1875, C1618 and to some  
244 extent to C1214, as well as with petro-diesel that generally consists of around 75% of paraffins and ~ 25% of unsaturated  
245 compounds (In the literature the average formula for diesel is C<sub>12</sub>H<sub>23</sub> (Heywood, 1988), corresponding to C<sub>12</sub> fuel but  
246 with no oxygen).

247 On the contrary fuels with higher oxygen content show an increase in the oxidative potential of the gas phase. This could be  
248 due to the vapor pressure of the oxidized gas phase compounds not being low enough to lead to the condensation onto the  
249 particle phase. By looking at the volatility change in respect to aging, it is obvious that the volatility increases upon  
250 exposure to UV and ozone for all the fuels. This may mean that in the case of short-chain, saturated biodiesels, aging leads  
251 to the condensation of certain species from the gas phase, which further increases OV, but does not carry any ROS potency.

252 The correlation between overall volatility of diesel particulate matter and the ROS can be seen in Figure 8. This figure  
253 shows the measured ROS levels and volatility of particulate matter for all the modes and blends both before and after  
254 aging. Blue markers are due to fresh particles and red markers are due to aged particulate matter. Particulate matter  
255 produced by each fuel is specified using a symbol as can be seen in the legends. This categorization method allows us to  
256 easily spot clusters of a color or a symbol. The first observation from Figure 8 is that the ROS correlates with OV. Note  
257 that the correlation is not linear but it is exponential. So a small increase in volatility of particulate matter can cause a  
258 significant increase in ROS levels. The symbols square and triangle are seen towards the righter and upper side of the  
259 figure, which again shows that more saturated fuels with shorter carbon chain length can cause more volatile and particles  
260 with a higher oxidative potential. It is also evident that blue markers tend to move toward the righter and upper side of the  
261 figure underlining the exacerbating effect of atmospheric aging on the biodiesel particulate matter.

#### 262 **4. Conclusion**

263 The objective of this research was to shed some light on the potential of biodiesel exhaust to generate SOA and to compare  
264 the potential toxicity of aged particles caused by biodiesel with that of petro-diesel. The results presented here showed that  
265 chemical composition of the fuel can affect the primary emissions as well as secondary emissions. Saturated fuels causing  
266 less PM also caused more volatile PM and significantly more semi volatiles in the gas phase with the potential to partition  
267 between the gas phase and particle phase upon aging. Moreover, aged particles from more saturated fuels with higher  
268 oxygen content have a higher oxidative potential as expressed through the increase of ROS concentration. Results of this  
269 research are in contrast with a few previous studies where it was claimed that use of biodiesel did not tend to increase the  
270 level of toxicity of diesel exhaust (Bagley et al., 1998;Jung et al., 2006;Jalava et al., 2012).

271 This study is not quantitative and cannot be used for SOA prediction within models. However, its qualitative analysis calls  
272 for the attention of regulating authorities and contributes to the overall body of knowledge on the effects of fuel  
273 composition on both engine primary as well as secondary emissions. Once emitted to the atmosphere, PM originating from

274 combusted biodiesel will transform and become more toxic than its parent molecules and its overall toxicity will mainly  
275 depend on the chemical properties of the fuel. Therefore categorizing all biodiesel fuels in one group, as it is in current  
276 regulations, may not be the most appropriate way of classification in respect to their emissions. Various biodiesel fuels are  
277 very different in terms of both physical properties and chemical compositions which combust differently causing  
278 substantially diverse species in the exhaust gases, particularly in PM and the semi-volatile fraction. Moreover, the exhaust  
279 gases from various biodiesel fuels behave differently when reacting with oxidative agents from the atmosphere. Perhaps  
280 new regulation should take some of the most important characteristics of the biodiesel into account and classify them in  
281 groups based on the oxygen content or level of saturation etc. Furthermore, current legislations only regulate the  
282 nonvolatile fraction of primary particles. There are no regulations for VOCs, semi-volatile matter and the capability of the  
283 emissions to form SOA (Giechaskiel et al., 2012). This study points out the necessity of redefining the legislations; and as  
284 experiments with flow-through reactors are more reproducible and less costly, they could be used for introduction of more  
285 stringent regulations.

## 286 5. Acknowledgments

287 The authors would like to acknowledge the support from the Australian Research Council under Grants LP110200158,  
288 DP1097125, DP130104904, DP110105535 and DP120100126. Laboratory assistance from Mr Noel Hartnett and Mr Scott  
289 Abbett were also appreciated.

## 290 6. References

- 291 Atkinson, R., Carter, W. P. L., Darnall, K. R., Winer, A. M., and Pitts, J. N.: A SMOG CHAMBER AND  
292 MODELING STUDY OF THE GAS-PHASE NOX-AIR PHOTO-OXIDATION OF TOLUENE AND THE CRESOLS,  
293 *International Journal of Chemical Kinetics*, 12, 779-836, 10.1002/kin.550121102, 1980.
- 294 Bagley, S. T., Gratz, L. D., Johnson, J. H., and McDonald, J. F.: Effects of an Oxidation Catalytic Converter  
295 and a Biodiesel Fuel on the Chemical, Mutagenic, and Particle Size Characteristics of Emissions from a  
296 Diesel Engine, *Environmental Science & Technology*, 32, 1183-1191, 10.1021/es970224q, 1998.
- 297 Biswas, S., Verma, V., Schauer, J. J., Cassee, F. R., Cho, A. K., and Sioutas, C.: Oxidative Potential of Semi-  
298 Volatile and Non Volatile Particulate Matter (PM) from Heavy-Duty Vehicles Retrofitted with Emission  
299 Control Technologies, *Environmental Science & Technology*, 43, 3905-3912, 10.1021/es9000592, 2009.
- 300 Cheng, C. H., Cheung, C. S., Chan, T. L., Lee, S. C., and Yao, C. D.: Experimental investigation on the  
301 performance, gaseous and particulate emissions of a methanol fumigated diesel engine, *Science of the  
302 Total Environment*, 389, 115-124, 10.1016/j.scitotenv.2007.08.041, 2008.
- 303 Cheung, K. L., Polidori, A., Ntziachristos, L., Tzamkiozis, T., Samaras, Z., Cassee, F. R., Gerlofs, M., and  
304 Sioutas, C.: Chemical Characteristics and Oxidative Potential of Particulate Matter Emissions from  
305 Gasoline, Diesel, and Biodiesel Cars, *Environmental Science & Technology*, 43, 6334-6340,  
306 10.1021/es900819t, 2009.

307 Chirico, R., DeCarlo, P. F., Heringa, M. F., Tritscher, T., Richter, R., Prevot, A. S. H., Dommen, J.,  
308 Weingartner, E., Wehrle, G., Gysel, M., Laborde, M., and Baltensperger, U.: Impact of aftertreatment  
309 devices on primary emissions and secondary organic aerosol formation potential from in-use diesel  
310 vehicles: results from smog chamber experiments, *Atmospheric Chemistry and Physics*, 10, 11545-  
311 11563, 10.5194/acp-10-11545-2010, 2010.

312 Donahue, N. M., Robinson, A. L., Stanier, C. O., and Pandis, S. N.: Coupled partitioning, dilution, and  
313 chemical aging of semivolatile organics, *Environmental Science & Technology*, 40, 2635-2643,  
314 10.1021/es052297c, 2006.

315 Fontaras, G., Karavalakis, G., Kousoulidou, M., Tzamkiozis, T., Ntziachristos, L., Bakeas, E., Stournas, S.,  
316 and Samaras, Z.: Effects of biodiesel on passenger car fuel consumption, regulated and non-regulated  
317 pollutant emissions over legislated and real-world driving cycles, *Fuel*, 88, 1608-1617,  
318 10.1016/j.fuel.2009.02.011, 2009.

319 Geiger, H., Kleffmann, J., and Wiesen, P.: Smog chamber studies on the influence of diesel exhaust on  
320 photo-smog formation, *Atmospheric Environment*, 36, 1737-1747, 10.1016/s1352-2310(02)00175-9,  
321 2002.

322 Giechaskiel, B., Alfoldy, B., and Drossinos, Y.: A metric for health effects studies of diesel exhaust  
323 particles, *Journal of Aerosol Science*, 40, 639-651, 10.1016/j.jaerosci.2009.04.008, 2009.

324 Giechaskiel, B., Mamakos, A., Andersson, J., Dilara, P., Martini, G., Schindler, W., and Bergmann, A.:  
325 Measurement of automotive nonvolatile particle number emissions within the European legislative  
326 framework: A review, *Aerosol Science and Technology*, 46, 719-749, 2012.

327 Heywood, J. B.: *Internal combustion engine fundamentals*, McGraw-hill New York, 1988.

328 Izumi, K., and Fukuyama, T.: PHOTOCHEMICAL AEROSOL FORMATION FROM AROMATIC-  
329 HYDROCARBONS IN THE PRESENCE OF NOX, *Atmospheric Environment Part a-General Topics*, 24, 1433-  
330 1441, 10.1016/0960-1686(90)90052-o, 1990.

331 Jalava, P. I., Aakko-Saksa, P., Murtonen, T., Happonen, M. S., Markkanen, A., Yli-Pirilä, P., Hakulinen, P.,  
332 Hillamo, R., Mäki-Paakkanen, J., and Salonen, R. O.: Toxicological properties of emission particles from  
333 heavy duty engines powered by conventional and bio-based diesel fuels and compressed natural gas,  
334 *Particle and fibre toxicology*, 9, 37, 10.1186/1743-8977-9-37, 2012.

335 Jathar, S. H., Miracolo, M. A., Tkacik, D. S., Donahue, N. M., Adams, P. J., and Robinson, A. L.: Secondary  
336 Organic Aerosol Formation from Photo-Oxidation of Unburned Fuel: Experimental Results and  
337 Implications for Aerosol Formation from Combustion Emissions, *Environmental Science & Technology*,  
338 47, 12886-12893, 10.1021/es403445q, 2013.

339 Johnson, G. R., Fletcher, C., Meyer, N., Modini, R., and Ristovski, Z.: A robust, portable H-TDMA for field  
340 use, *Journal of Aerosol Science*, 39, 850-861, 2008.

341 Jung, H., Kittelson, D. B., and Zachariah, M. R.: Characteristics of SME Biodiesel-Fueled Diesel Particle  
342 Emissions and the Kinetics of Oxidation, *Environmental Science & Technology*, 40, 4949-4955,  
343 10.1021/es0515452, 2006.

344 Kalligeros, S., Zannikos, F., Stournas, S., Lois, E., Anastopoulos, G., Teas, C., and Sakellariopoulos, F.: An  
345 investigation of using biodiesel/marine diesel blends on the performance of a stationary diesel engine,  
346 *Biomass and Bioenergy*, 24, 141-149, 2003.

347 Kang, E., Root, M. J., Toohey, D. W., and Brune, W. H.: Introducing the concept of Potential Aerosol Mass  
348 (PAM), *Atmos. Chem. Phys.*, 7, 5727-5744, 10.5194/acp-7-5727-2007, 2007.

349 Keller, A., and Burtscher, H.: A continuous photo-oxidation flow reactor for a defined measurement of  
350 the SOA formation potential of wood burning emissions, *Journal of Aerosol Science*, 49, 9-20,  
351 10.1016/j.jaerosci.2012.02.007, 2012.

352 Knothe, G., Sharp, C. A., and Ryan III, T. W.: Exhaust emissions of biodiesel, petrodiesel, neat methyl  
353 esters, and alkanes in a new technology engine, *Energy & Fuels*, 20, 403-408, 2006.

354 Kroll, J. H., and Seinfeld, J. H.: Chemistry of secondary organic aerosol: Formation and evolution of low-  
355 volatility organics in the atmosphere, *Atmospheric Environment*, 42, 3593-3624,  
356 10.1016/j.atmosenv.2008.01.003, 2008.

357 Lambe, A. T., Ahern, A. T., Williams, L. R., Slowik, J. G., Wong, J. P. S., Abbatt, J. P. D., Brune, W. H., Ng, N.  
358 L., Wright, J. P., Croasdale, D. R., Worsnop, D. R., Davidovits, P., and Onasch, T. B.: Characterization of  
359 aerosol photooxidation flow reactors: heterogeneous oxidation, secondary organic aerosol formation  
360 and cloud condensation nuclei activity measurements, *Atmos. Meas. Tech.*, 4, 445-461, 10.5194/amt-4-  
361 445-2011, 2011.

362 Lee, S., Jang, M., and Kamens, R. M.: SOA formation from the photooxidation of  $\alpha$ -pinene in the  
363 presence of freshly emitted diesel soot exhaust, *Atmospheric Environment*, 38, 2597-2605,  
364 10.1016/j.atmosenv.2003.12.041, 2004.

365 Leskinen, A. P., Jokinen, J. K., and Lehtinen, K. E. J.: Transformation of diesel engine exhaust in an  
366 environmental chamber, *Atmospheric Environment*, 41, 8865-8873, 10.1016/j.atmosenv.2007.08.021,  
367 2007.

368 Li, Q., Wyatt, A., and Kamens, R. M.: Oxidant generation and toxicity enhancement of aged-diesel  
369 exhaust, *Atmospheric Environment*, 43, 1037-1042, 10.1016/j.atmosenv.2008.11.018, 2009.

370 Lipsky, E. M., and Robinson, A. L.: Effects of dilution on fine particle mass and partitioning of semivolatile  
371 organics in diesel exhaust and wood smoke, *Environmental Science & Technology*, 40, 155-162,  
372 10.1021/es050319p, 2006.

373 Liu, Y. Y., Lin, T. C., Wang, Y. J., and Ho, W. L.: Biological toxicities of emissions from an unmodified  
374 engine fueled with diesel and biodiesel blend, *Journal of Environmental Science and Health Part a-  
375 Toxic/Hazardous Substances & Environmental Engineering*, 43, 1735-1743,  
376 10.1080/10934520802330438, 2008.

377 McWhinney, R. D., Gao, S. S., Zhou, S. M., and Abbatt, J. P. D.: Evaluation of the Effects of Ozone  
378 Oxidation on Redox-Cycling Activity of Two-Stroke Engine Exhaust Particles, *Environmental Science &  
379 Technology*, 45, 2131-2136, 10.1021/es102874d, 2011.

380 Miljevic, B., Modini, R. L., Bottle, S. E., and Ristovski, Z. D.: On the efficiency of impingers with fritted  
381 nozzle tip for collection of ultrafine particles, *Atmospheric Environment*, 43, 1372-1376, DOI:  
382 10.1016/j.atmosenv.2008.12.001, 2009.

383 Miljevic, B., Heringa, M. F., Keller, A., Meyer, N. K., Good, J., Lauber, A., Decarlo, P. F., Fairfull-Smith, K.  
384 E., Nussbaumer, T., Burtscher, H., Prevot, A. S. H., Baltensperger, U., Bottle, S. E., and Ristovski, Z. D.:  
385 Oxidative Potential of Logwood and Pellet Burning Particles Assessed by a Novel Profluorescent  
386 Nitroxide Probe, *Environmental Science & Technology*, 44, 6601-6607, 10.1021/es100963y, 2010.

387 Miracolo, M. A., Presto, A. A., Lambe, A. T., Hennigan, C. J., Donahue, N. M., Kroll, J. H., Worsnop, D. R.,  
388 and Robinson, A. L.: Photo-Oxidation of Low-Volatility Organics Found in Motor Vehicle Emissions:  
389 Production and Chemical Evolution of Organic Aerosol Mass, *Environmental Science & Technology*, 44,  
390 1638-1643, 10.1021/es902635c, 2010.

391 Miracolo, M. A., Hennigan, C. J., Ranjan, M., Nguyen, N. T., Gordon, T. D., Lipsky, E. M., Presto, A. A.,  
392 Donahue, N. M., and Robinson, A. L.: Secondary aerosol formation from photochemical aging of aircraft  
393 exhaust in a smog chamber, *Atmospheric Chemistry and Physics*, 11, 4135-4147, 10.5194/acp-11-4135-  
394 2011, 2011.

395 Nakao, S., Shrivastava, M., Nguyen, A., Jung, H. J., and Cocker, D.: Interpretation of Secondary Organic  
396 Aerosol Formation from Diesel Exhaust Photooxidation in an Environmental Chamber, *Aerosol Science  
397 and Technology*, 45, 964-974, 10.1080/02786826.2011.573510, 2011.

398 Pey, J., Querol, X., Alastuey, A., Rodríguez, S., Putaud, J. P., and Van Dingenen, R.: Source apportionment  
399 of urban fine and ultra-fine particle number concentration in a Western Mediterranean city,  
400 *Atmospheric Environment*, 43, 4407-4415, 2009.

401 Pourkhesalian, A. M., Stevanovic, S., Salimi, F., Rahman, M., Wang, H., Pham, P. X., Bottle, S. E., Masri,  
402 A., Brown, R. J., and Ristovski, Z. D.: Influence of Fuel Molecular Structure on the Volatility and Oxidative  
403 Potential of Biodiesel Particulate Matter, *Environmental Science & Technology*, 48, 12577-12585, 2014.  
404 Rahman, M. M., Pourkhesalian, A. M., Jahirul, M. I., Stevanovic, S., Pham, P. X., Wang, H., Masri, A. R.,  
405 Brown, R. J., and Ristovski, Z. D.: Particle emissions from biodiesels with different physical properties  
406 and chemical composition, *Fuel*, 134, 201-208, <http://dx.doi.org/10.1016/j.fuel.2014.05.053>, 2014.  
407 Robinson, A. L., Donahue, N. M., Shrivastava, M. K., Weitkamp, E. A., Sage, A. M., Grieshop, A. P., Lane,  
408 T. E., Pierce, J. R., and Pandis, S. N.: Rethinking organic aerosols: Semivolatile emissions and  
409 photochemical aging, *Science*, 315, 1259-1262, 10.1126/science.1133061, 2007.  
410 Rönkkö, T., Virtanen, A., Vaaraslahti, K., Keskinen, J., Pirjola, L., and Lappi, M.: Effect of dilution  
411 conditions and driving parameters on nucleation mode particles in diesel exhaust: Laboratory and on-  
412 road study, *Atmospheric Environment*, 40, 2893-2901, 10.1016/j.atmosenv.2006.01.002, 2006.  
413 Samy, S., and Zielinska, B.: Secondary organic aerosol production from modern diesel engine emissions,  
414 *Atmospheric Chemistry and Physics*, 10, 609-625, 2010.  
415 Shi, J. P., and Harrison, R. M.: Investigation of Ultrafine Particle Formation during Diesel Exhaust  
416 Dilution, *Environmental Science & Technology*, 33, 3730-3736, 10.1021/es981187l, 1999.  
417 Sidhu, S., Graham, J., and Striebich, R.: Semi-volatile and particulate emissions from the combustion of  
418 alternative diesel fuels, *Chemosphere*, 42, 681-690, 10.1016/s0045-6535(00)00242-3, 2001.  
419 Stevanovic, S., Miljevic, B., Eaglesham, G. K., Bottle, S. E., Ristovski, Z. D., and Fairfull-Smith, K. E.: The  
420 Use of a Nitroxide Probe in DMSO to Capture Free Radicals in Particulate Pollution, *European Journal of*  
421 *Organic Chemistry*, 2012, 5908-5912, 10.1002/ejoc.201200903, 2012a.  
422 Stevanovic, S., Ristovski, Z. D., Miljevic, B., Fairfull-Smith, K. E., and Bottle, S. E.: APPLICATION OF  
423 PROFLUORESCENT NITROXIDES FOR MEASUREMENTS OF OXIDATIVE CAPACITY OF COMBUSTION  
424 GENERATED PARTICLES, *Chemical Industry & Chemical Engineering Quarterly*, 18, 653-659,  
425 10.2298/ciceq120113113s, 2012b.  
426 Stevanovic, S., Miljevic, B., Surawski, N. C., Fairfull-Smith, K. E., Bottle, S. E., Brown, R., and Ristovski, Z.  
427 D.: Influence of Oxygenated Organic Aerosols (OOAs) on the Oxidative Potential of Diesel and Biodiesel  
428 Particulate Matter, *Environmental Science & Technology*, 47, 7655-7662, 10.1021/es4007433, 2013.  
429 Surawski, N. C., Miljevic, B., Ayoko, G. A., Roberts, B. A., Elbagir, S., Fairfull-Smith, K. E., Bottle, S. E., and  
430 Ristovski, Z. D.: Physicochemical Characterization of Particulate Emissions from a Compression Ignition  
431 Engine Employing Two Injection Technologies and Three Fuels, *Environmental Science & Technology*, 45,  
432 5498-5505, 10.1021/es200388f, 2011.  
433 Surawski, N. C., Miljevic, B., Bodisco, T. A., Brown, R. J., Ristovski, Z. D., and Ayoko, G. A.: Application of  
434 Multicriteria Decision Making Methods to Compression Ignition Engine Efficiency and Gaseous,  
435 Particulate, and Greenhouse Gas Emissions, *Environmental Science & Technology*, 47, 1904-1912,  
436 10.1021/es3035208, 2013.  
437 Tinsdale, M., Price, P., and Chen, R.: The impact of biodiesel on particle number, size and mass emissions  
438 from a Euro4 diesel vehicle, 2010.  
439 Verma, V., Ning, Z., Cho, A. K., Schauer, J. J., Shafer, M. M., and Sioutas, C.: Redox activity of urban quasi-  
440 ultrafine particles from primary and secondary sources, *Atmospheric Environment*, 43, 6360-6368,  
441 10.1016/j.atmosenv.2009.09.019, 2009.  
442 Wang, J., Doussin, J. F., Perrier, S., Perraudin, E., Katrib, Y., Pangui, E., and Picquet-Varrault, B.: Design of  
443 a new multi-phase experimental simulation chamber for atmospheric photosmog, aerosol and cloud  
444 chemistry research, *Atmos. Meas. Tech.*, 4, 2465-2494, 10.5194/amt-4-2465-2011, 2011.  
445 Weitkamp, E. A., Sage, A. M., Pierce, J. R., Donahue, N. M., and Robinson, A. L.: Organic aerosol  
446 formation from photochemical oxidation of diesel exhaust in a smog chamber, *Environmental Science &*  
447 *Technology*, 41, 6969-6975, 10.1021/es070193r, 2007.  
448 Wickham, H.: *ggplot2: elegant graphics for data analysis*, Springer, 2009.

449 World Health Organization: Outdoor air pollution a leading environmental cause of cancer deaths, IARC  
450 scientific publications, 1-4, 2013.

451 Xu, Z., Li, X., Guan, C., and Huang, Z.: Characteristics of Exhaust Diesel Particles from Different  
452 Oxygenated Fuels, *Energy & Fuels*, 7579–7586, 10.1021/ef401946t, 2013.

453 Zielinska, B.: Atmospheric transformation of diesel emissions, *Experimental and Toxicologic Pathology*,  
454 57, 31-42, 10.1016/j.etp.2005.05.006, 2005.

455

## 456 7. List of figures

457 **Fig. 1** Experiment setup HEPA: High-Efficiency Particulate Air Filter; F T reactor: Flow-Trough Reactor; O3 Gen:  
458 Ozone Generator; Ozone Analyser: EC9810 Ecotech; EC: Electrostatic Classifier; TD: Thermo-Denuder; VTDMA:  
459 Volatility Tandem Differential Mobility Analyser; CPC: Condensation Particle Counter; SMPS: Scanning Mobility  
460 Particle Sizer; Impingers: used to collect DPM for ROS measurements.

461 **Fig. 2** the volumetric volatile fraction (v<sub>vf</sub>) of particles versus particle pre-selection sizes for different biodiesels and  
462 different blends before and after aging. Each column is dedicated to one of the biodiesels and each row specifies one  
463 blend. Red markers represent the particles before aging and blue markers show the particles after aging. Error bars  
464 show the SEM for V-TDMA. All the tests were carried out at quarter load, 1500rpm.

465 **Fig. 3** volatility of particulate matter versus different blends for petro-diesel and tested biodiesels before and after  
466 aging in the flow through reactor. Blue points are due to aged particulate matter and red points represent fresh  
467 particles. Different tested biodiesels can be seen at the top of the figure. B0 representing petro-diesel is repeated in  
468 all graphs for comparison.

469 **Fig. 4** change in volatility of particles before and after aging against oxygen content of the blends. Different blends  
470 are shown with colours and different shapes as can be seen in the legend show different fuels. The point  
471 corresponding to C1875, B100 is excluded from the model. The grey area shows the 95% confidence interval of the  
472 fit.  $R^2 = 0.66$

473 **Fig. 5** ROS levels of particulate matter versus different blends for petro-diesel and tested biodiesels before aging  
474 (red circles) and after aging (blue triangles). Different tested biodiesels can be seen at the top of the figure. B0  
475 representing petro-diesel is repeated in all graphs for comparison.

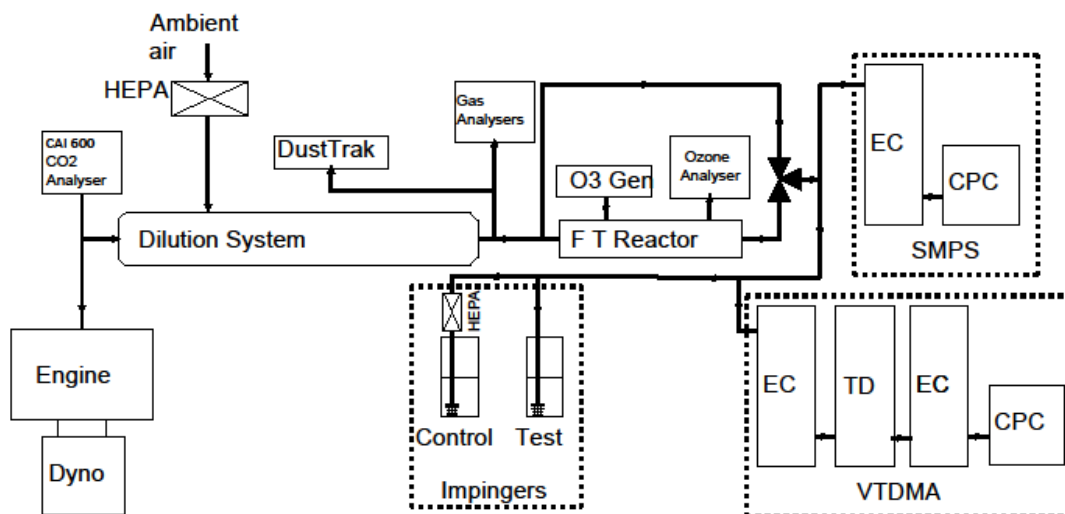


476 **Fig. 6** the correlation between the change in ROS levels and oxygen content the fuels before and after aging . The  
477 point corresponding to C1875 is excluded from the model. The grey area shows the 95% confidence interval of the  
478 fit.  $R^2= 0.55$

479 **Fig. 7** ROS levels in gas phase before and after aging. Fresh and aged particulate matter are separated using blue  
480 color for aged PM and red for fresh PM.

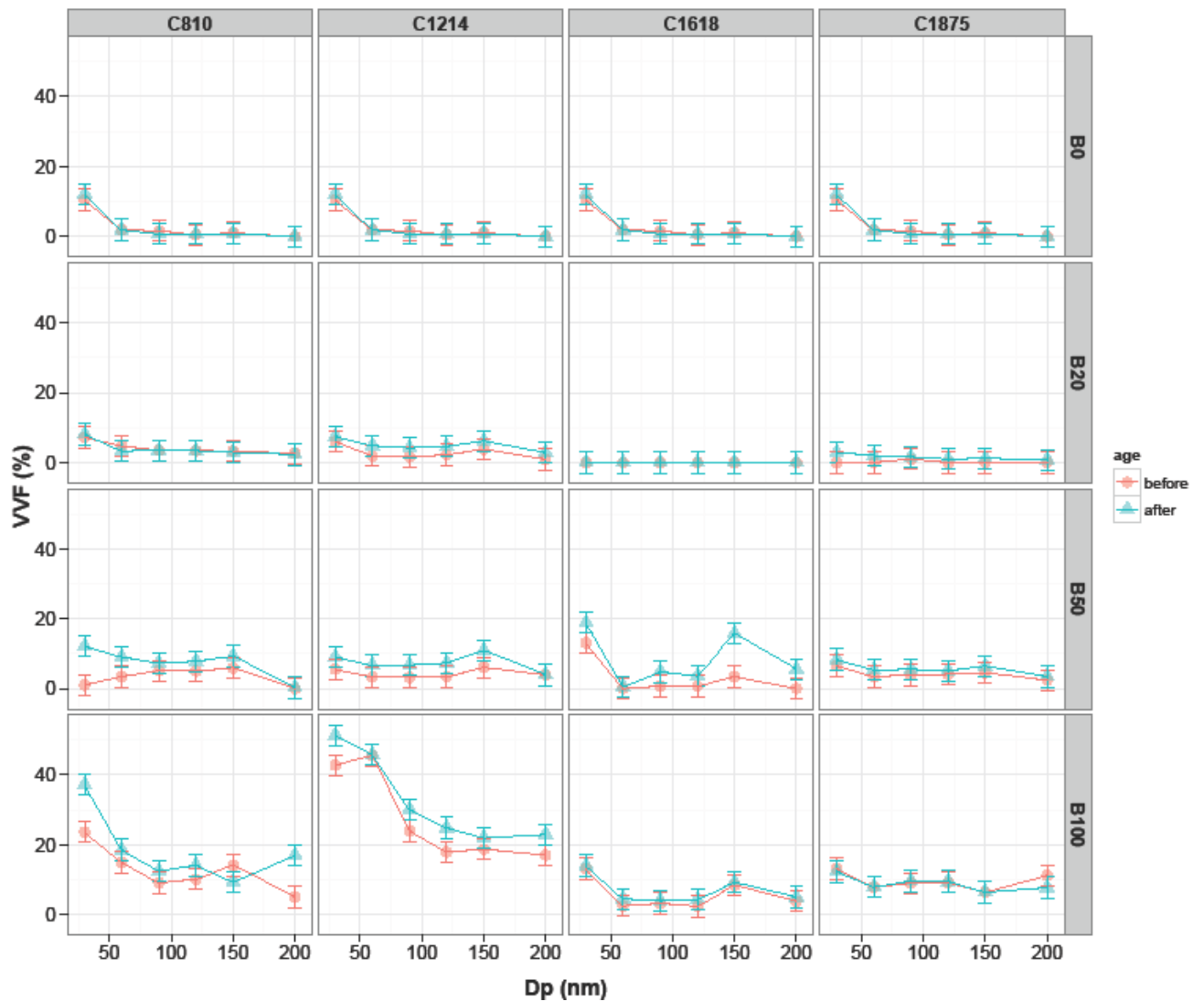
481 **Fig. 8** the correlation between ROS of particulate matter and the volatility of particulate matter. Fresh and aged  
482 particulate matter are separated using blue color for fresh PM and red for aged PM, also the shape of the markers  
483 represents different fuel. The grey area shows the 95% confidence interval of the fit.  $R^2= 0.86$

484



485 Fig. 1 Experiment setup HEPA: High-Efficiency Particulate Air Filter; F T reactor: Flow-Trough Reactor; O3 Gen:  
 486 Ozone Generator; Ozone Analyser: EC9810 Ecotech; EC: Electrostatic Classifier; TD: Thermo-Denuder; VTDMA:  
 487 Volatility Tandem Differential Mobility Analyser; CPC: Condensation Particle Counter; SMPS: Scanning Mobility  
 488 Particle Sizer; Impingers: used to collect DPM for ROS measurements.

490



492

493

Fig. 2 the volumetric volatile fraction (vvf) of particles versus particle pre-selection sizes for different biodiesels and

494

different blends before and after aging. Each column is dedicated to one of the biodiesels and each row specifies one

495

blend. Red markers represent the particles before aging and blue markers show the particles after aging. Error bars

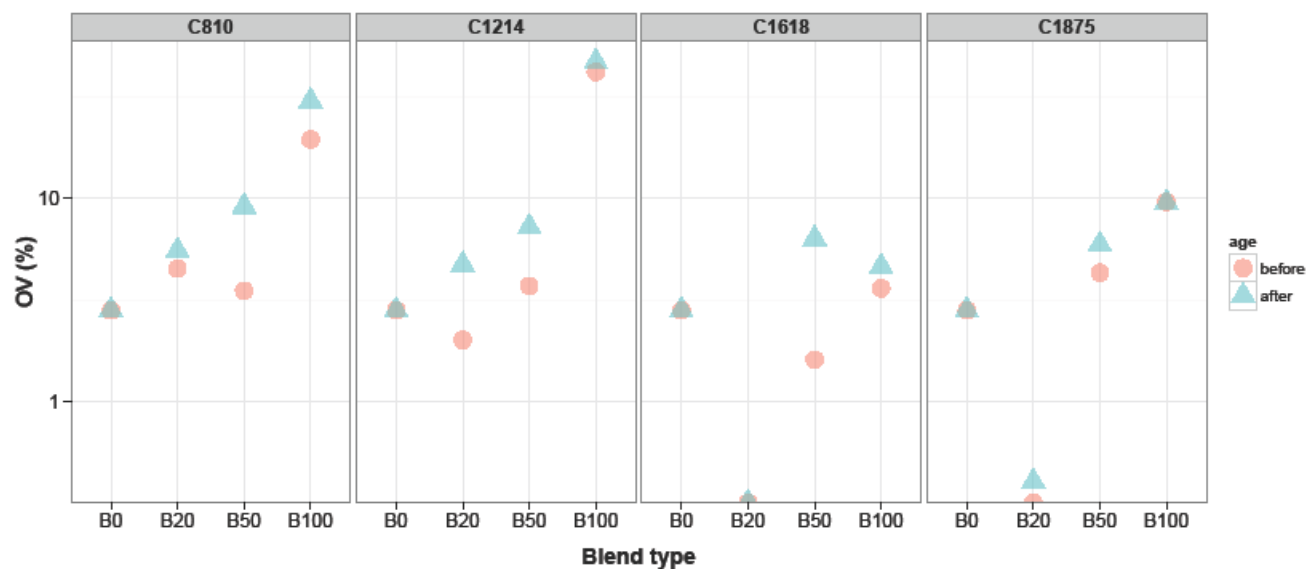
496

show the SEM for V-TDMA. All the tests were carried out at quarter load, 1500rpm.

497

498

499



500

501 Fig. 3 Volatility of particulate matter versus different blends for petro-diesel and tested biodiesels before and after

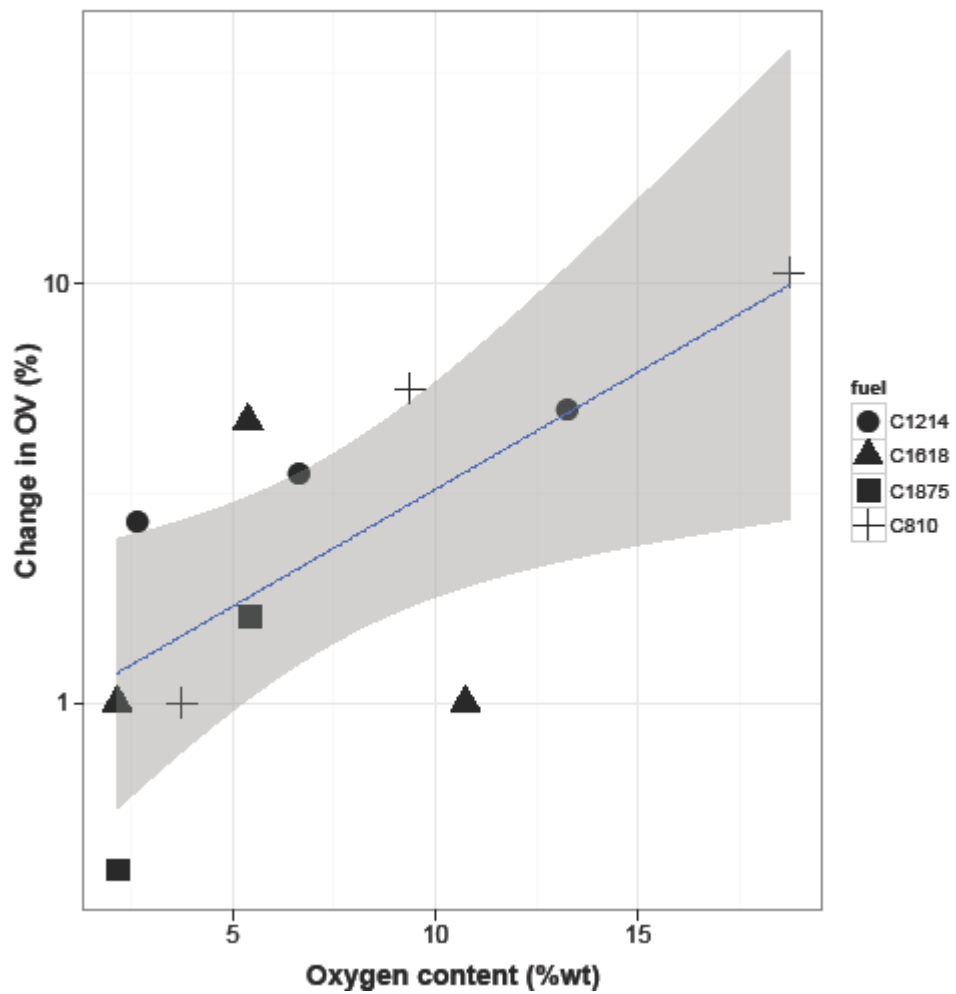
502 aging in the flow through reactor. Blue points are due to aged particulate matter and red points represent fresh

503 particles. Different tested biodiesels can be seen at the top of the figure. B0 representing petro-diesel is repeated in

504 all graphs for comparison

505

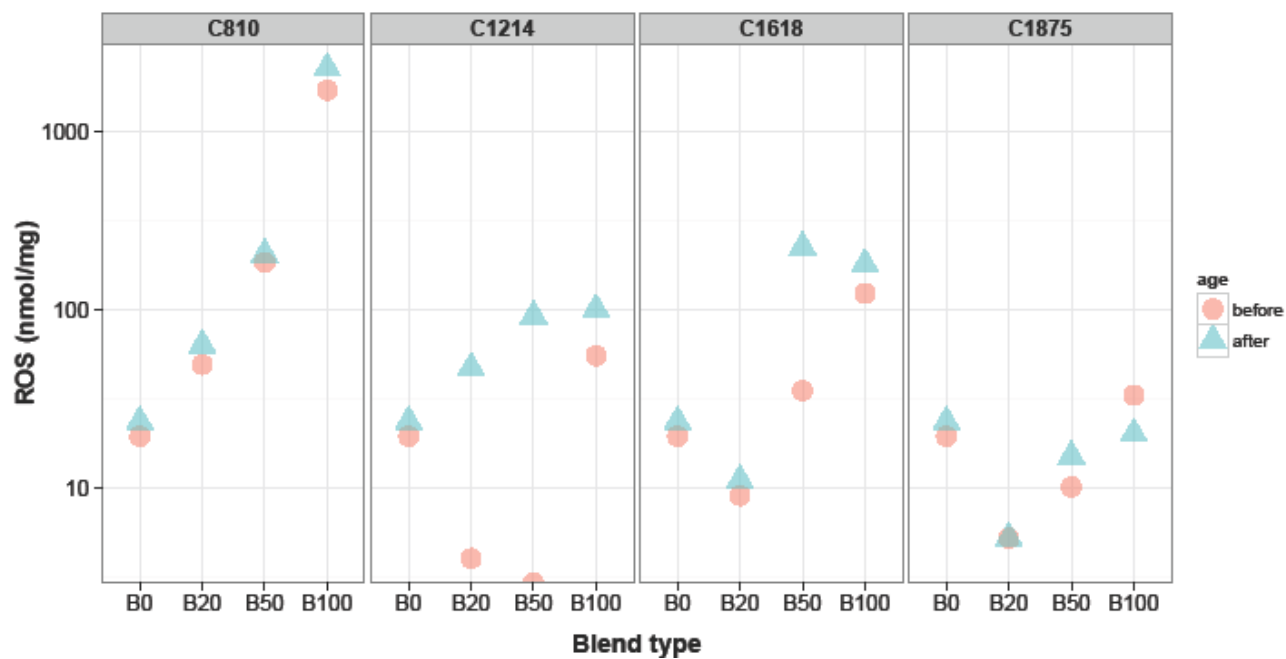
506



507

508 Fig. 4 change in volatility of particles before and after aging against oxygen content of the blends. Different blends  
509 are shown with colours and different shapes as can be seen in the legend show different fuels. The point  
510 corresponding to C1875, B100 is excluded from the model. The grey area shows the 95% confidence interval of the  
511 fit.  $R^2=0.66$

512



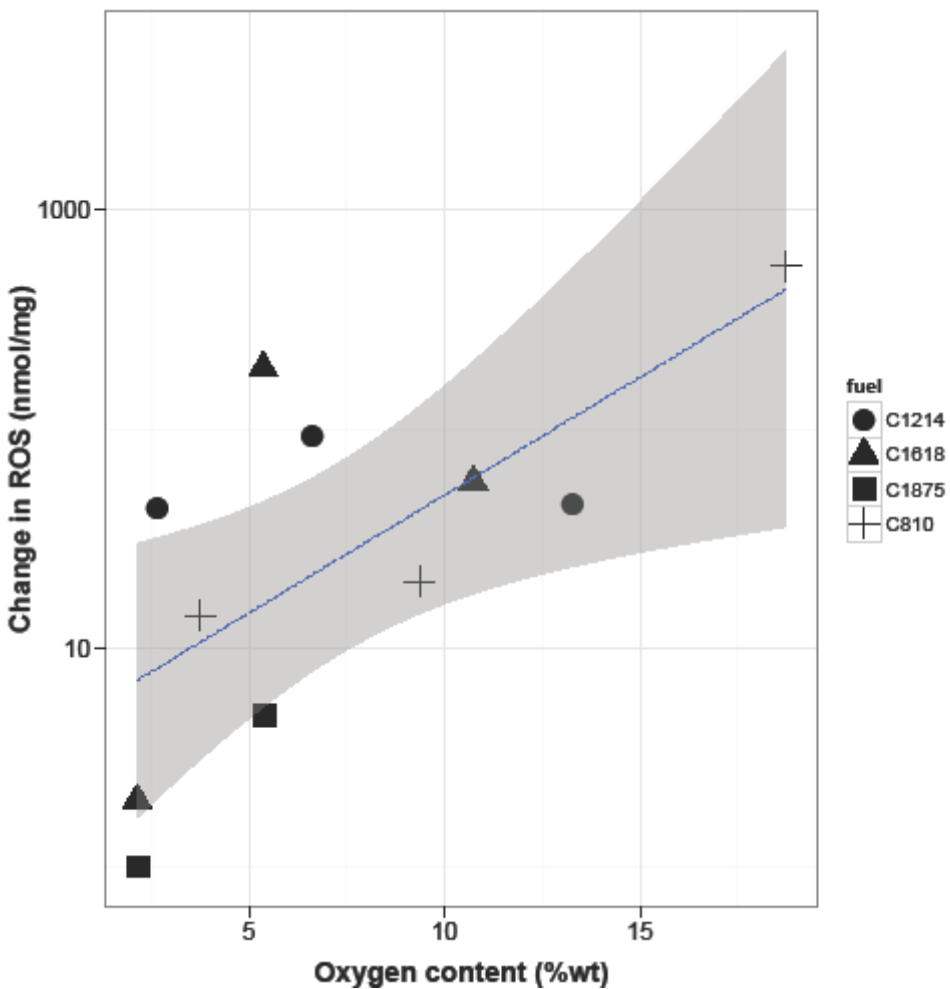
514

515 Fig. 5 ROS levels of particulate matter versus different blends for petro-diesel and tested biodiesels before aging

516 (red circles) and after aging (blue triangles). Different tested biodiesels can be seen at the top of the figure. B0

517 representing petro-diesel is repeated in all graphs for comparison.

518

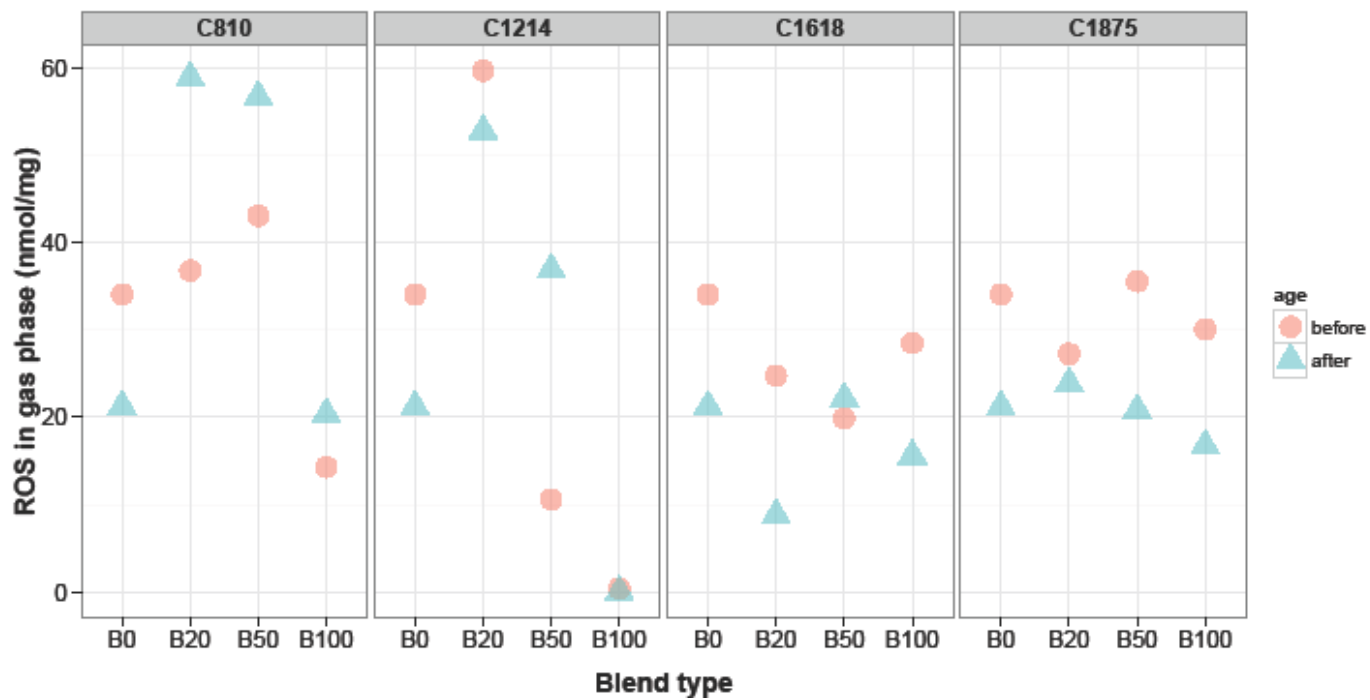


520

521 Fig. 6 the correlation between the change in ROS levels and oxygen content the fuels before and after aging . The  
522 point corresponding to C1875 is excluded from the model. The grey area shows the 95% confidence interval of the  
523 fit.  $R^2 = 0.52$

524

525



526

527 Fig. 7 ROS levels in gas phase before and after aging. Fresh and aged particulate matter are separated using blue

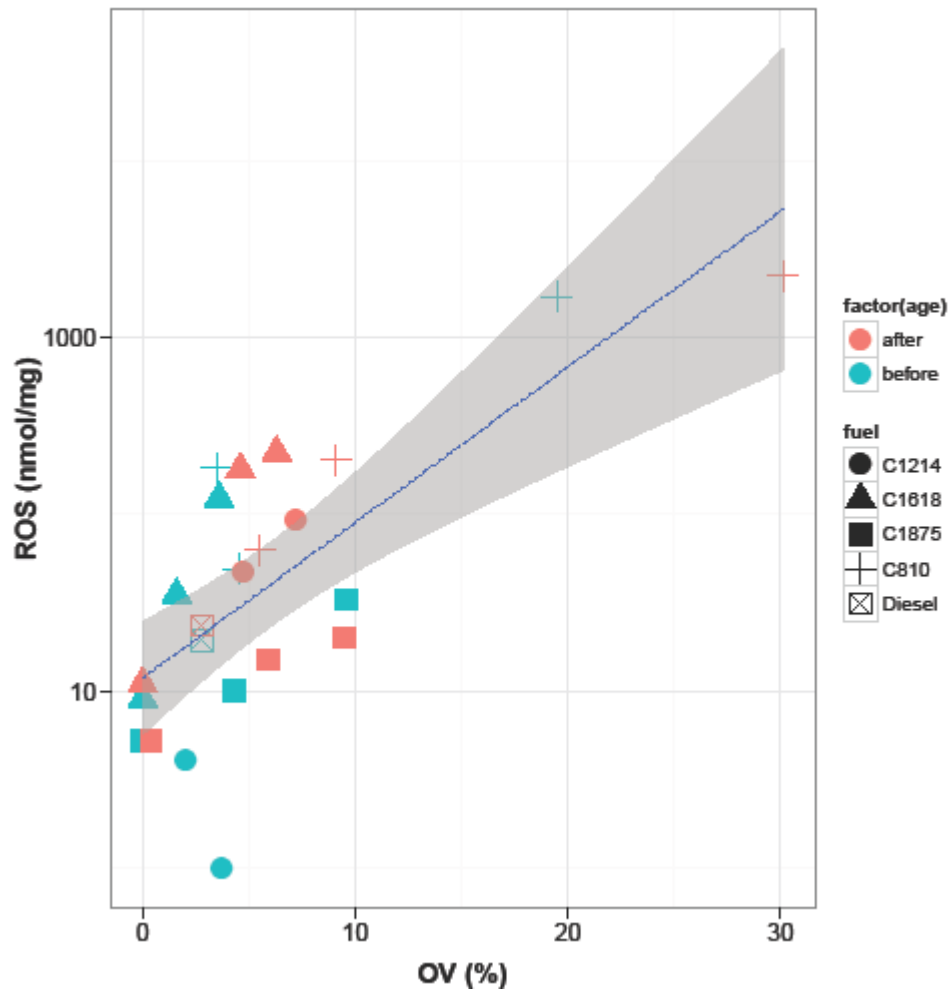
528

color for aged PM and red for fresh PM

529



530



531

532 Fig. 8 the correlation between ROS of particulate matter and the volatility of particulate matter. Fresh and aged

533 particulate matter are separated using blue color for fresh PM and red for aged PM, also the shape of the markers

534 represents different fuel. The grey area shows the 95% confidence interval of the fit.  $R^2= 0.86$